NEUROSCIENCE

Social place-cells in the bat hippocampus

David B. Omer, Shir R. Maimon, Liora Las,*† Nachum Ulanovsky*†

Social animals have to know the spatial positions of conspecifics. However, it is unknown how the position of others is represented in the brain. We designed a spatial observational-learning task, in which an observer bat mimicked a demonstrator bat while we recorded hippocampal dorsal-CA1 neurons from the observer bat. A neuronal subpopulation represented the position of the other bat, in allocentric coordinates. About half of these "social place-cells" represented also the observer's own position—that is, were place cells. The representation of the demonstrator bat did not reflect self-movement or trajectory planning by the observer. Some neurons represented also the position of inanimate moving objects; however, their representation differed from the representation of the demonstrator bat. This suggests a role for hippocampal CA1 neurons in social-spatial cognition.

It is important for social animals to know the spatial position of conspecifics, for purposes of social interactions, observational learning, and group navigation. Decades of research on the mammalian hippocampal formation has revealed a set of spatial neurons that represent self-position and orientation, including place cells (*1*–*3*), grid cells (*4*–*6*), head-direction cells (*7*–*9*), and border/boundary cells (*10*–*12*). However, it remains unknown how the location of other animals is represented in the brain.

We designed an observational-learning task for Egyptian fruit bats (*Rousettus aegyptiacus*), which are highly social mammals that live in colonies with complex social structures (*13*). Bats were trained in pairs: In each trial, one bat ("observer") had to remain stationary on a "start ball" and to observe and remember the flight trajectory of the other bat ("demonstrator"), which was flying roughly randomly to one of two landing balls (Fig. 1A,"demonstrator flying" in trials *i* and *j*). After a delay, the observer bat had to imitate the demonstrator bat and fly to the same landing ball to receive a reward (Fig. 1A, "observer flying," and movies S1 and S2). This task had two key features: First, it required the observer to pay close attention to the demonstrator's position and to hold this position in memory during the delay period (the average delay between the demonstrator's return to the start ball and the observer's takeoff was rather long: 12.7 ± 8.6 s; mean ± SD). Second, because the observer was stationary during the demonstrator's flight, it allowed temporal dissociation between the effects of self-flights versus the flights of the other bat.

While the bats performed the task, we recorded the activity of 378 single neurons in the dorsal hippocampal area CA1 of four observer bats, using a wireless electrophysiology system (Fig. 1B) (*14*). For each neuron, we computed two firing-rate maps: a "classical" map, based on the self-movement flight trajectories of the observer—the standard depiction for place cells (Fig. 1C, "Self," left map for each neuron)—and a nonclassical map based on the spikes recorded from the observer's neuron together with the demonstrator's flight trajectories (Fig. 1C, "Demo," right maps) (*14*). We focused our analysis on the two-dimensional horizontal projections because the bats' flights were confined mostly to a narrow horizontal slab around the height of the landing balls (fig. S1). A subpopulation of hippocampal CA1 neurons encoded the position of the demonstrator-bat (Fig. 1C, cells 358, 254, 52, and 266—the right map in each example—and fig. S2). We termed these neurons "social place-cells."

We classified 68 of the 378 recorded CA1 neurons (18.0%) as significant social place-cells—significantly encoding the position of the other bat—based on spatial information (95th percentile in a shuffling analysis) (*14*). Using the same criteria, 261 of the 378 recorded neurons (69.0%) significantly encoded the self-position of the observer bat when it was flying and were thus classified as place cells (Fig. 1D). Of the 261 place cells, 14.9% were also social place-cells. Conversely, of the 68 social place-cells, 57.4% (39 neurons) were also place cells (Fig. 1, C—cells 358, 254, 52—and D), whereas the remaining 29 social place-cells (42.6%) were not place cells. Most of these neurons (16 of 29 cells; 55.2%) became completely inactive during self-flights, although they encoded the conspecific's position on interleaved demonstrator flights (examples are provided in Fig. 1C, cell 266, and fig. S2, cells 229 and 60).

This new type of social-spatial representation exhibited several features that were similar to the standard place cell representation: Both representations showed directional selectivity (Fig. 1E and fig. S3), and both place cells and social place-cells tiled space rather uniformly (Fig. 1F). However, we found also clear differences between the two representations: First, the firing rates of the social place-cells were significantly lower than for the classical place-cells (unpaired *t* test, $P < 0.01$) (Fig. 1G) [firing-rates of classical place cells were similar to our previous report from CA1 of flying bats (*15*)]. Second, in the 39 cells that encoded both self-position and conspecific position—were both place cells and social place-cells—we found a wide range of correlation values between the representations for self and other. Some neurons exhibited high similarity between their place field and social place field ("congruent cells," with positive correlations) (fig. S2, cells 68 and 45), whereas in other neurons, the place field and social place field were dissimilar ("noncongruent cells," with negative correlations) (Fig. 1C, cells 358 and 254, and fig. S2, cell 242). Overall, we found a continuum from noncongruent to congruent representations (Fig. 1H, top histograms), but we also found a slight overrepresentation of congruent cells among higher-firing neurons (Fig. 1H, bottom, gray bars, and top right histogram). These data suggest partial remapping between the hippocampal representations of self-position and conspecific-position, which can be interpreted as reflecting the contextual difference between observing a conspecific versus self-movement.

Next, we sought to rule out the possibility that social place fields might result from the observer's head movements during the demonstrator's flights. We therefore recorded head acceleration and head azimuth using a nine-axis motion-sensor that was placed on the observer's head (*14*). When the demonstrator bat was flying, the observer bat hardly moved its head: There was a lack of changes in head acceleration of the observer bat during the flights of the demonstrator bat (Fig. 2A, middle and bottom, gray areas). Consistent with this, in most of the demonstrator flights, the head azimuth of the observer changed by less than 20°, which is equivalent to a very small head movement of less than 6 mm (Fig. 2, B—black traces and rightmost *y* axis, in magenta—and C). Such small head movements did not modulate the firing of social place-cells outside the task (Fig. 2D). These bats have a wide visual field and no fovea (*13*) and hence did not need to move their head in order to track the demonstrator. However, in some of the demonstrator flights (35.4%), the observer bat did move its head more than 20° (the value of 20° corresponds roughly to ± 1 SD in azimuth) (Fig. 2, B, gray traces and C, gray vertical lines). These deviant flights might have potentially modulated the firing of the neurons. To rule out this possibility, we recomputed the social firing-rate maps after excluding the deviant flights and found that these maps were very similar to the original maps (Fig. 2, E, examples, and F, population analysis).

A second potential interpretation is that social place fields may reflect planning of the upcoming flight trajectory by the observer bat. To rule out this possibility, we conducted three analyses. (i) Trajectory planning by hippocampal cell assemblies has been linked to sharp-wave-ripples (SWRs) (*16*). We recorded the local field potential (LFP) in the observer bat, then detected SWRs (Fig. 2, G and H) and tested whether removing the observer flights that contained SWRs would affect social place fields (Fig. 2, I and J) (*14*). The removal of these flights hardly affected the social place field

Department of Neurobiology, Weizmann Institute of Science, Rehovot 76100, Israel.
*These authors contributed equally to this work.
†Corresponding author. Email: nachum.ulanovsky@weizmann.ac.il (N.U.); liora.las@weizmann.ac.il (L.L.)

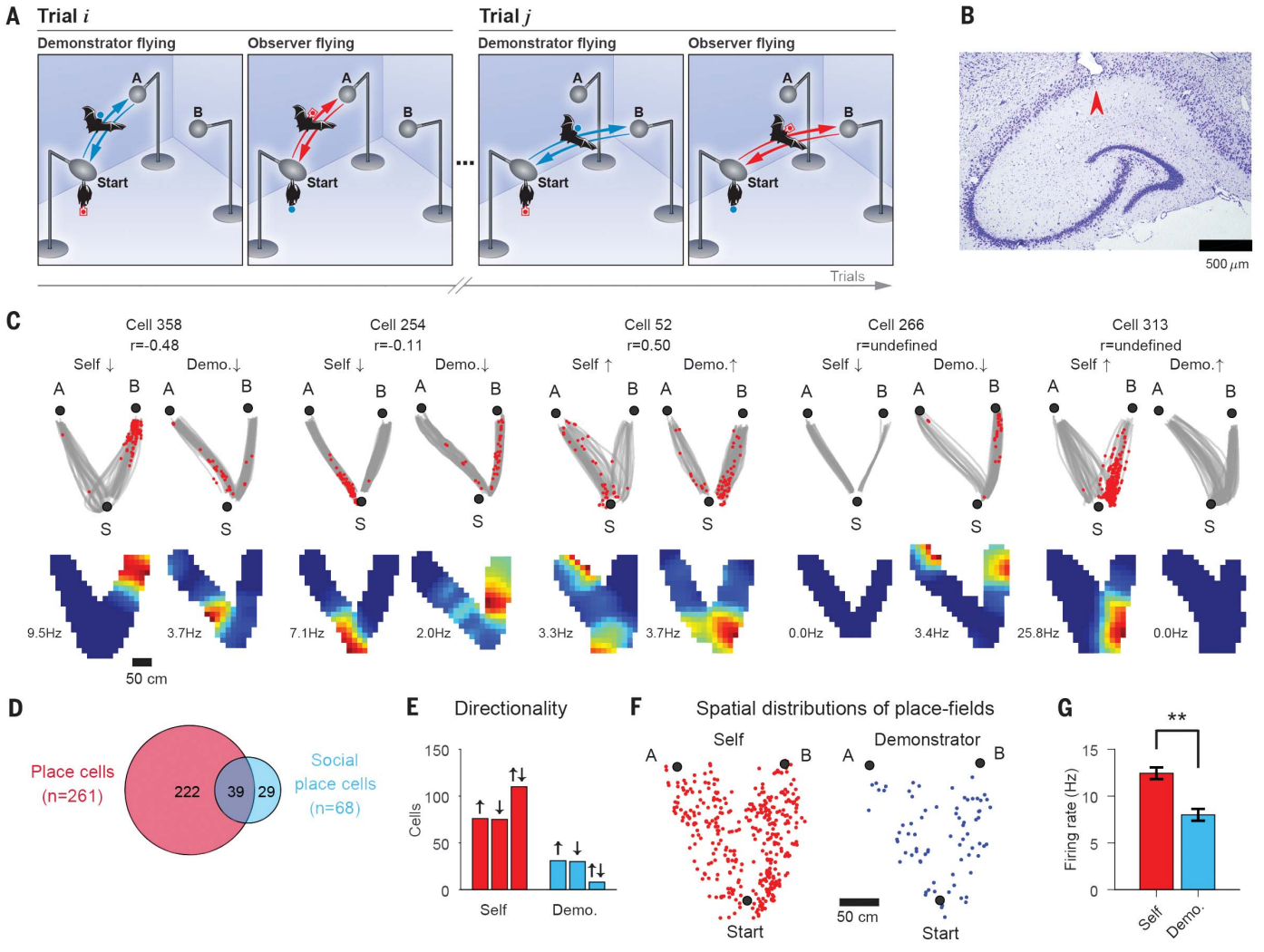

Fig. 1. Neurons in bat hippocampal area CA1 represent the position of conspecifics. (**A**) Behavioral setup inside a flight room (2.30 by 2.69 by 2.56 m). The demonstrator bat (blue) was trained to fly from the start ball, roughly randomly to either ball A or ball B, and back, and the observer bat had to imitate this flight. Two different trials are shown, one to ball A (trial *i*) and one to ball B (trial *j*). (**B**) Coronal section through dorsal hippocampus of one observer bat. Arrowhead, electrolytic lesion at end of tetrode track. (**C**) Five example cells (top view). For each cell, the left column shows the place-cell representation, based on spikes from the observer's neuron and the self-flight-trajectories of the observer (Self), and the right column shows the social place-cell representation, based on spikes from the same observer's neuron, plotted together with the demonstrator's trajectories (Demo.). (Top) Flight trajectories (gray) with spikes overlaid (red). A, B, and S are landing balls A, B, and start ball; arrows denote flight-direction (↑, flying away from start-ball; ↓, flying toward the start ball). (Bottom) Firing-rate maps. Color scale ranges from zero (blue) to maximal firing rate (red; value indicated). The four leftmost cells are social place-cells; some of these neurons are also place-cells (cells 358, 254, and 52), and some are not (cell 266). Cell 313 is a "pure" place cell. Correlations between the firing-rate maps for self and other are indicated for each cell (correlations are undefined for cells 266 and 313 because one of the maps is flat). Scale bar, 50 cm. (**D**) Total number of significant social place-cells versus significant classical place cells that we recorded. (**E**) Number of place cells and social place-cells that were significantly tuned to one flight-direction (↑), the other flight-direction (↓), or both directions (↑↓). Classical place cells are in red (n = 261), and social place-cells are in blue (n = 68). (**F**) Locations of peak firing for all the significant maps for place cells (red dots, n = 371 cells × directions), and social place-cells (blue dots, n = 76 cells × directions); cells that had significant tuning in both directions were depicted twice; hence, the counts here are larger than in (D). Dots were randomly jittered by up to ±5 cm (half bin) for display purposes. (**G**) Average peak firing rate for all the classical place cells (red, n = 371 cells × directions) and all the social place-cells (blue, n = 76 cells × directions). $^{**}P < 0.01$. (**H**) (Top) Distributions of correlation coefficients between classical place cell maps and social place-cell maps for all the neurons that encoded significantly either self-position or conspecific position and had >20 spikes per map (left histogram) or >300 spikes per map (right histogram). Gray, the data; black lines, cell-shuffling distributions (*14*). (Bottom) Map correlations increased with firing rate. Error bars, mean ± SEM; gray bars, the data; open bars, cell-shuffling; number of cells × directions included in the four bars: n = 334, 218, 137, and 91; $^{*}P < 0.05$; $^{**}P < 0.01$; n.s., nonsignificant.

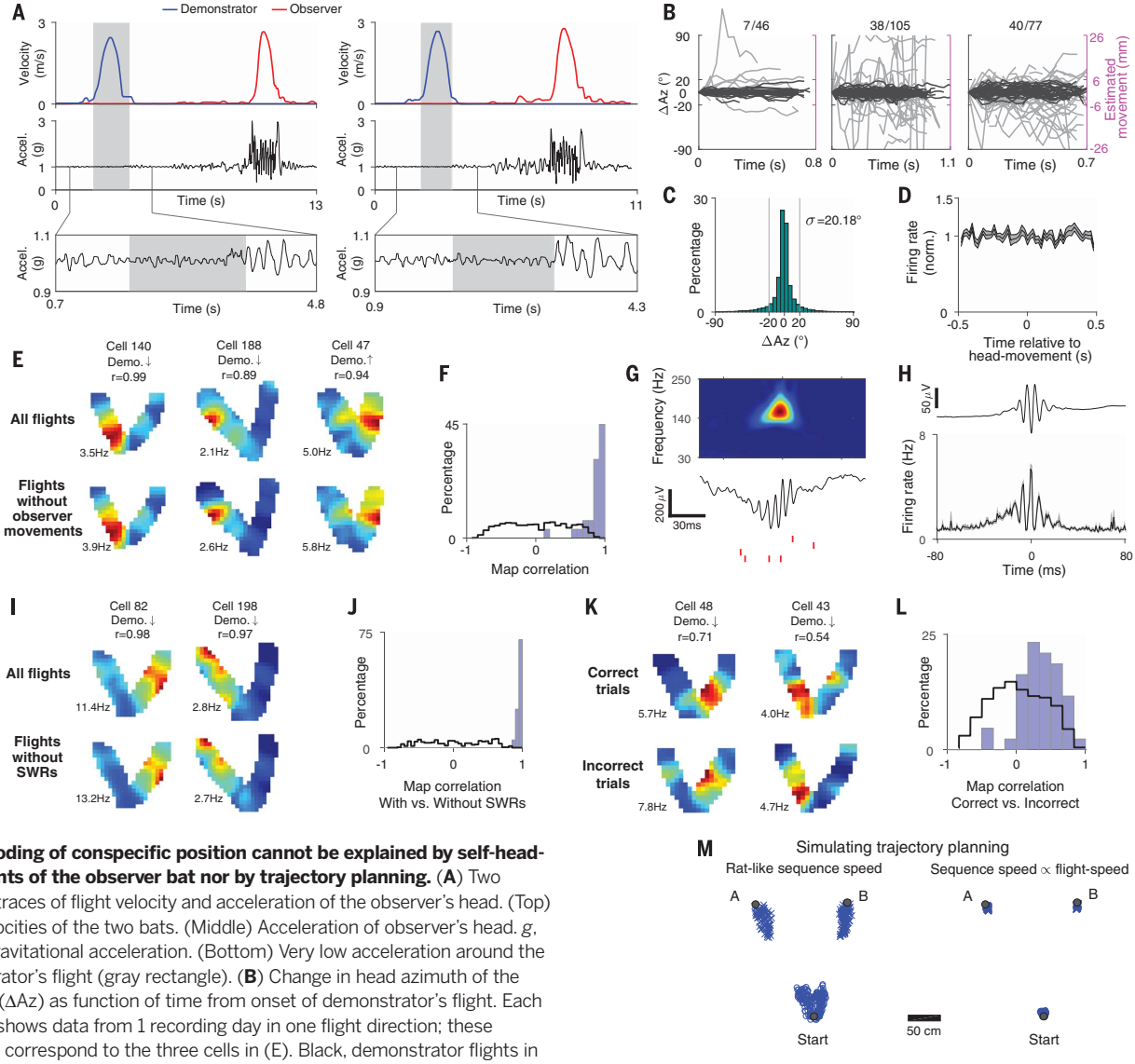

Fig. 2. Coding of conspecific position cannot be explained by self-head-movements of the observer bat nor by trajectory planning. (**A**) Two example traces of flight velocity and acceleration of the observer's head. (Top) Flight velocities of the two bats. (Middle) Acceleration of observer's head. *g*, Earth's gravitational acceleration. (Bottom) Very low acceleration around the demonstrator's flight (gray rectangle). (**B**) Change in head azimuth of the observer (ΔAz) as function of time from onset of demonstrator's flight. Each example shows data from 1 recording day in one flight direction; these examples correspond to the three cells in (E). Black, demonstrator flights in which the observer's head moved <1 SD (σ = 20.18°, which corresponds to <6 mm movement; right *y* axis) (*14*). Gray, demonstrator flights that included deviant head movements of the observer bat that exceeded ±σ. Numbers indicate proportion of deviant flights out of all the flights on this day. (**C**) Distribution of ΔAz of the observer's head, pooled over all days with significant social place-cells where motion-sensor data were recorded (n = 18 days, n = 35,284 samples). Gray lines mark 1 SD (σ = 20.18 °), which was the threshold used in (B) to define deviant flights. (**D**) Mean firing rate of social place-cells outside the task, triggered on the peak velocity of observer's head movements, for all the 1-s segments with small angular displacement <20° (n = 14,893 segments, pooled over all significant social place-cells with motion-sensor data; shaded area indicates mean ± SEM). (**E**) Three example cells, showing high correlation between social place field maps before (top) and after (bottom) removal of all the flights that included observer head-movements [At bottom, we removed all gray-colored flights in (B) and the corresponding spikes]. (**F**) Blue histogram, distribution of correlation coefficients between social place-cell maps with and without removal of flights with observer movements. Black line, cell-shuffling distribution. We included here all the significant social place-cells where motion-sensor data were recorded (n = 29 cells × directions). Shown are high correlations between maps with versus without removal of flights with observer movements (blue histogram); t test with unequal variances, compared with cell-shuffling control (black): $P < 10^{-26}$. (**G**) Example of a SWR. (Top) Spectrogram of the SWR. (Middle) Raw LFP trace (1 to 400 Hz bandpass). Scale bars, 30 ms and 200 μV. (Bottom) Spikes from four simultaneously recorded neurons (red ticks). Same time scale in all panels. (**H**) (Top) Mean SWR waveform, averaged across all recording days with social place-cells (n = 46 days; n = 9,092 SWRs). (Bottom) SWR-triggered firing rate, averaged over all neurons recorded during days with social place-cells (n = 276 neurons; shaded area, mean ± SEM). (**I**) Two social place-cells (columns), showing high stability with versus without flights that included SWRs (top versus bottom). (**J**) Distribution of correlation coefficients between social place-cell maps and the same maps after removal of flights with SWRs. Blue histogram, data for all cells with >20 spikes per map that had SWRs during observer flights (n = 20 cells × directions). Black line, cell-shuffling distribution. t test with unequal variances, data compared with cell-shuffling control: $P < 10^{-140}$. (**K**) Two social place-cells (columns), showing high stability in correct trials (top) versus incorrect trials (bottom). (**L**) Distribution of correlation coefficients between social place-cell maps computed by using correct trials versus incorrect trials. Blue histogram, data for all neurons with >20 spikes per map (n = 43 cells × directions). Black line, cell-shuffling distribution. t test with unequal variances, data compared with cell-shuffling control: $P < 10^{-8}$. We included in this analysis only cells with >15 correct flights and >15 incorrect flights; n = 43 cells × directions. (**M**) (Left) Simulated spatial distribution of social place fields, assuming that they are generated by place cell sequences with a ratlike sequence-speed of 8 m/s (*14*). (Right) Same, using a sequence speed of 43 m/s, which is scaled up to the flight speed of the demonstrator bat (corresponding to 20 times the bat's flight speed in our task). Blue circles and crosses denote cells with preferred direction ↑ and ↓, respectively.

maps, as indicated by very high map-correlations (Fig. 2, I, examples, and J, population), suggesting that social place fields are not created by SWR-associated trajectory planning. (ii) Next, we analyzed the neuronal activity during correct versus incorrect trials because studies in rats showed that hippocampal cell-assembly activity is strongly correlated to choice behavior on correct/incorrect trials (*17*). We reasoned that if the firing of the neurons reflects planning, then there would be a difference between social place-cell maps computed by using correct versus incorrect trials (where "incorrect" means that the demonstrator's flight was followed by an incorrect flight of the observer)—because before incorrect flights, the observer bat is likely planning to fly to the opposite landing ball from the demonstrator. However, we found high correlations between correct-trial maps and incorrect-trial maps (Fig. 2, K, examples, and L, population). (iii) Trajectory planning has been linked to hippocampal place cell sequences (*16*), and such sequences might potentially create the social place fields that we observed. However, this seems highly unlikely because place cell sequences play extremely rapidly—at a speed of 8 m/s in rats (*18*), which is ~20 times faster than the running speed of the animal (*18*)—and therefore, all the firing of the observer's neurons would be spatially compressed in one location, such as immediately after the takeoff of the demonstrator (*14*). Indeed, simulations of place-cell sequences confirmed this: All the place fields in this simulation were spatially compressed near the takeoff balls (Fig. 2M, blue crosses and circles), unlike the experimentally observed uniform distribution of social place fields (Fig. 1F, right). Together, this argues that social place fields cannot be explained via trajectory planning by the observer bat. Moreover, if trajectory planning in the observer's brain is somehow synchronized precisely to the timing and velocity of each of the demonstrator's flights—which seems rather unlikely—then it constitutes an explicit spatial representation of the position of the other bat.

Classical place cells in CA1 represent the animal's self-position in a world coordinate-frame: "allocentric coordinates" (*1*). To test whether social place-cells also form an allocentric representation, we exploited the fact that although the bats did not move their head much during the demonstrator flights (Fig. 2, A to C), the head did point in different azimuthal directions across different flights (we focused here on the azimuthal angle because the observer bats mainly moved their head in azimuth) (Fig. 3, A and B, and fig. S4) (*14*). For each of the social place-cells, we computed the median head azimuth of the observer (Fig. 3B, red line) and then used this median to divide all the demonstrator's flights into two halves, corresponding to the observer bat looking right versus looking left (Fig. 3C, top versus bottom, respectively). If social place-cells are allocentric, then we expect similar maps irrespective of the head azimuth of the observer. Indeed, maps computed during right-viewing and left-viewing were rather similar (Fig. 3, C, examples, and D, population), which is consistent with an allocentric representation. Further, there was no relation between the map correlation and the average head direction difference between looking right and looking left [correlation coefficient (r) = −0.12, P = 0.59; the head-direction differences spanned a broad range, from ΔAz = 30° to 102°] (Fig. 3E and fig. S4), which also is consistent with an allocentric representation. These neurons are thus fundamentally different from vectorial goal-direction cells in the bat hippocampus, which represent the direction to navigational goals in egocentric coordinates (*19*).

Last, we asked whether a flying conspecific is represented differently from inanimate moving objects. We conducted additional experiments in two of the four recorded bats. These experiments included three sessions (Fig. 4A). Session 1 was conducted as before (Fig. 1A). In session 2, we moved an object either to ball A or to ball B, and the observer bat had to imitate it; it was the same task as before, but with an object instead of a conspecific. We termed this object an "informative object" (Fig. 4A, session 2, and fig. S5B) (*14*). In session 3, the observer bat was trained to hang at a fixed position on the start ball and to do nothing, while we moved a different object, a "noninformative object" (in this session, the observer bat did not receive reward and hence did not fly) (Fig. 4A, session 3, and fig. S5C). Both objects were similar in size to a flying bat (fig. S5). Surprisingly, we found quite a few CA1 cells that encoded the position of inanimate moving objects (Fig. 4, B, four top examples, and C, population); to our knowledge, this is the first report that the position of moving objects is explicitly represented in the hippocampus [a previous study reported modulation of place cell firing by the movement of another object, but not an explicit spatial representation of that object (*20*)]. Some of the CA1 cells represented both the inanimate objects and the conspecific (Fig. 4B, cells 184, 169, and 361); some cells represented only the objects (Fig. 4B, cell 182); and some cells represented only the conspecific (Fig. 4B, cell 221 and C, population summary). There were some differences between the representations of the conspecific and the inanimate objects. First, there was a slight trend for a better encoding of space (higher spatial information) going from the demonstrator bat to the informative object and to the noninformative object (Wilcoxon rank-sum tests, informative object versus noninformative object, P < 0.05; demonstrator bat versus noninformative-object, P = 0.093; demonstrator bat versus informative-object, P = 0.824; Kruskal-Wallis test, P = 0.092) (Fig. 4D). Second, whereas the representation of

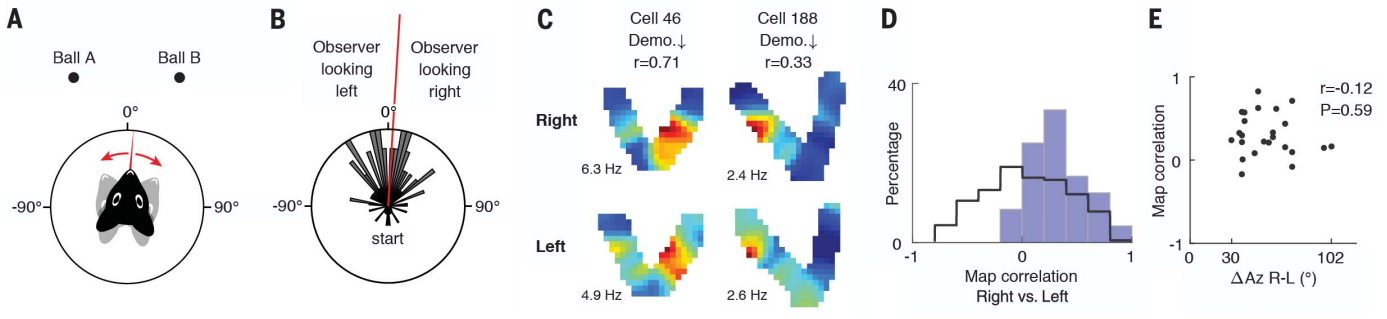

Fig. 3. The representation of conspecifics is allocentric, not egocentric. (**A** and **B**) Dividing the demonstrator's flight data based on the observer's head direction during demonstrator's flights. (A) Schematic drawing of directional notations of the bat's head relative to the two landing balls. (B) Distribution of the azimuthal head directions of the observer during demonstrator flights; data from 1 recording day. The median head direction (6.8°) is plotted in red. Direction 0° is parallel to the east-west wall of the room. (**C**) Two cells showing stability of their social place fields between right-pointing head directions (top) and left-pointing head directions (bottom). (**D**) Blue histogram, distribution of the correlation coefficients between right-looking maps and left-looking maps (blue), plotted for all the social place-cells for which we recorded motion-sensor data and had >20 spikes per map (n = 24 cells × directions); t test with unequal variances, compared with cell-shuffling control (black): $P < 10^{-4}$. Black line, cell-shuffling distribution, consisting of correlations between left-looking maps from cell i and right-looking maps from cell j across all the cell pairs where $i \neq j$. (**E**) Scatter plot of the similarity between right-looking and left-looking maps (y axis), versus the difference between the means of the right-looking and left-looking angles (x axis). No correlation was found (r = −0.12, P = 0.59; shown is a large span of azimuthal head-direction angles).

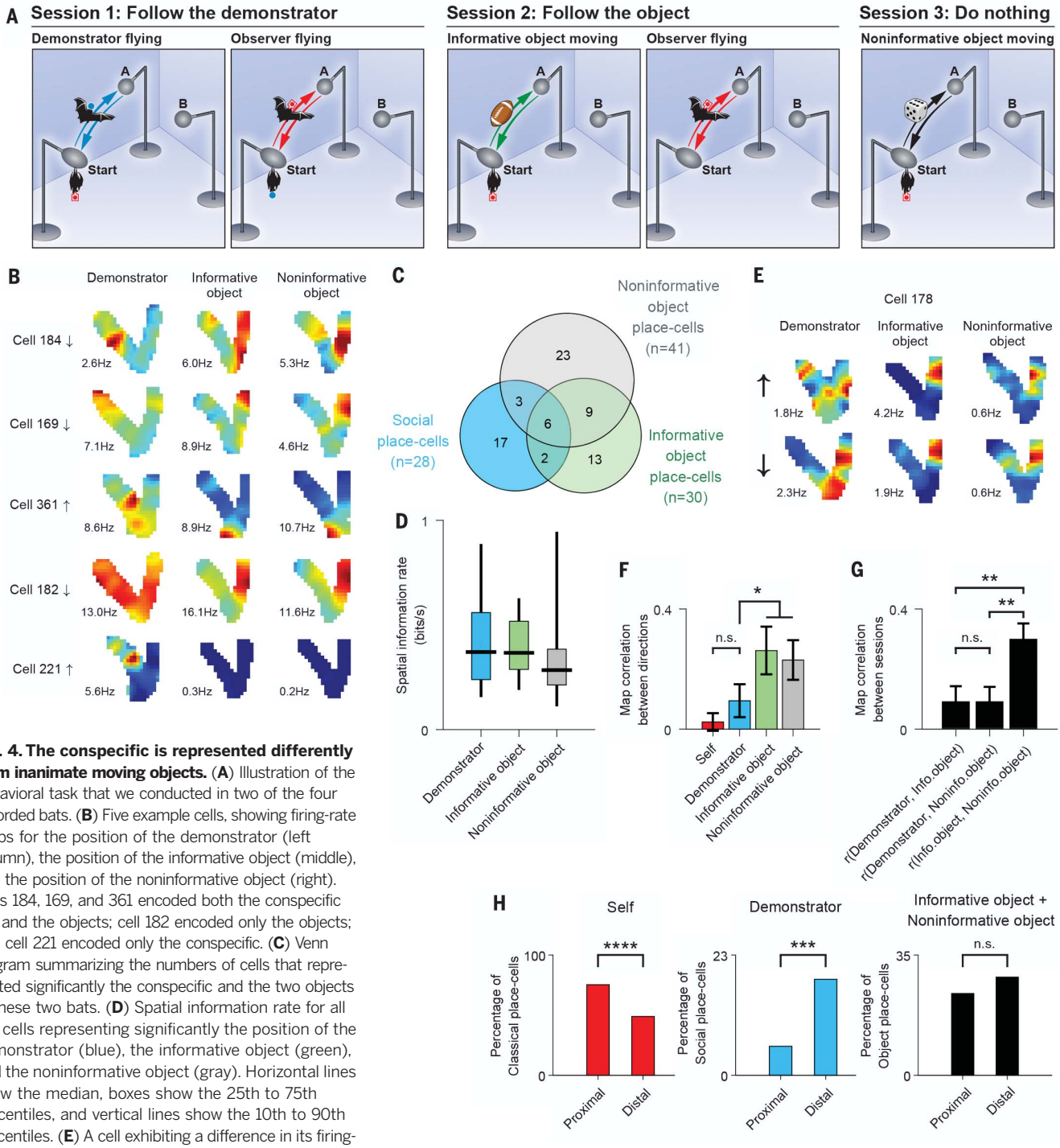

Fig. 4. The conspecific is represented differently from inanimate moving objects. (**A**) Illustration of the behavioral task that we conducted in two of the four recorded bats. (**B**) Five example cells, showing firing-rate maps for the position of the demonstrator (left column), the position of the informative object (middle), and the position of the noninformative object (right). Cells 184, 169, and 361 encoded both the conspecific bat and the objects; cell 182 encoded only the objects; and cell 221 encoded only the conspecific. (**C**) Venn diagram summarizing the numbers of cells that represented significantly the conspecific and the two objects in these two bats. (**D**) Spatial information rate for all the cells representing significantly the position of the demonstrator (blue), the informative object (green), and the noninformative object (gray). Horizontal lines show the median, boxes show the 25th to 75th percentiles, and vertical lines show the 10th to 90th percentiles. (**E**) A cell exhibiting a difference in its firing-rate maps between different flight directions of the demonstrator bat (left column), but showing no directionality for the two objects (middle and right columns); compare the top and bottom maps for the two objects (direction ↑ vs ↓). (**F**) Directionality: population summary. Shown are correlations of firing-rate maps between the two flight directions: for the self-representation, the demonstrator bat, and the informative and noninformative objects (data for all cells in which at least one flight direction exhibited a significant map, and both maps contained >50 spikes per map). The maps are much more directional (lower correlations) for the demonstrator than for the two objects; *t* test for the correlations between the two directions for demonstrator-bat versus the two pooled objects: $*P < 0.05$. (**G**) Correlations of firing-rate maps for demonstrator bat versus informative object (left), demonstrator bat versus noninformative object (middle), and informative object versus noninformative object (right). Correlations here were computed for all cells in which at least one of the two maps was significant, and only for maps with >50 spikes; *t* test of the object-object similarity versus the conspecific-object similarities: $**P < 0.01$ for both comparisons. To increase the robustness of comparisons between demonstrator and objects, (C), (D), (F), and (G) included only cells that met a strict criterion of >25 flights per map and >50 spikes per map. (**H**) Functional anatomy along the proximodistal axis of CA1, for one of the two bats tested with three sessions (*14*). Shown is the percentage of significant tuning, separately for proximal and distal tetrodes. (Left) Place cells (Self). (Middle) Social place-cells (Demonstrator). (Right) Object place cells (pooled over both objects). $***P < 10^{-3}$; $****P < 10^{-5}$.

the conspecific was directional—akin to the directionality exhibited by self place fields—the representation of both objects was nondirectional, that is, rather similar in both directions (Fig. 4, E, example, and F, population). Third, the representation of the demonstrator bat was significantly less similar to any of the object representations, as compared with the similarity between the two object representations (Fig. 4, B, cells 184,169, and 361; E, examples of similar firing for both objects; and G, population) (controls for spatial-coverage, velocity, and firing-rate are provided in fig. S6). Fourth, we found a significant difference in the functional-anatomical gradient between social place-cells and object place cells, along the proximodistal axis of CA1. Social place-cells were significantly more prevalent closer to the distal border of CA1 (log odds-ratio test: $P < 10^{-3}$) (Fig. 4H, middle, and fig. S7) (*14*), unlike object place-cells, which did not exhibit a significant proximodistal gradient (log odds-ratio test: $P = 0.17$) (Fig. 4H, right). Social place-cells exhibited the opposite pattern from classical place cells, which—consistent with previous reports in rats (*21*)—were significantly more prevalent near the proximal border of CA1 (log odds-ratio test: $P < 10^{-5}$) (Fig. 4H, left). However, this result (Fig. 4H) was obtained from a single animal (out of the two bats tested in all three sessions), in which we had a sufficient number of neurons and good proximodistal span of tetrodes (*14*); future studies will need to examine this in more detail. Together, these results suggest that the representation of the conspecific is rather different from the representation of inanimate objects, indicating that the spatial coding of the conspecific is not a simple sensory response driven by any sensory stimulus that moves through the social place field. Rather, these are context-dependent cognitive representations.

We found in this work a subpopulation of cells in bat dorsal CA1 that encode the position of conspecifics, in allocentric coordinates. This representation could not be explained by self-head-movements or by self-trajectory-planning. The responses to the conspecific were directional, which is in line with the directionality of classical place cells, but can also be interpreted through the social difference between an approaching and receding conspecific. Social place fields are unlikely to reflect either distance-coding (observer-demonstrator distance) or time-coding (time since demonstrator-takeoff) because in both cases, we would expect rather symmetric firing fields on flights to both ball A and ball B, whereas nearly all the social place-cells had a firing field on one side only. However, an alternative interpretation is that these neurons encode a position-by-time signal: Namely, they encode the spatial side to which the demonstrator bat is flying, together with its time from takeoff. We also found qualitative differences between the spatial representations of conspecifics versus inanimate moving objects. The different encoding of conspecifics versus objects may arise from (partially) different mechanisms. For example, spatial representation of moving objects in CA1 might arise from convergence of spatial inputs from grid cells in the medial entorhinal cortex (*4*, *6*) and object-related inputs from neurons in the lateral entorhinal cortex (*22*, *23*); by contrast, social place-cells may also involve socially modulated inputs from CA2 (*24*, *25*). Future studies are thus needed in order to search for social place-cells in the bat CA2, medial, and lateral entorhinal cortices, as well as in the ventral CA1, which was recently shown to be important for social memory (*26*).

It may seem surprising that social place-cells were not discovered previously in several studies of rat hippocampus that looked for a modulation of classical place fields by the presence of conspecifics (*27*–*29*). We believe that the key difference is in the task: In those previous studies, there was no incentive for the animal to pay attention to the position of the conspecific; our task, in contrast, required the bat to pay close attention to the position of the other bat and to hold this position in memory during a 12.7-s average delay, which revealed a spatial representation for the other. This interpretation is consistent with many studies that showed that hippocampal representations are highly task-dependent, plastic, and memory-dependent (*30*–*32*). Additionally, this task created a high level of social interactions between the two bats: When the bats were together at the start ball, they often approached and touched each other and emitted many social vocalizations (fig. S8), and this intensely social situation may have contributed to the representation of the conspecific.

There is an apparent similarity between the social place-cells, which encode the position of the other, and "mirror neurons" in monkeys, which encode the actions of the other (*33*). One difference, however, is that noncongruent social place-cells (Fig. 1C, cells 358 and 254) are still useful functionally because they encode meaningful information about the position of the other, whereas it is less clear how noncongruent mirror neurons in monkeys might be useful for the proposed functions of mirror neurons. Thus, social place-cells are conceptually different from mirror neurons, although both might possibly share a similar functional principle, whereby the same neuronal circuit can be used for self-representation as well as for representing conspecifics.

Last, we speculate that social place-cells may play a role in a wide range of social behaviors in many species—from group navigation and coordinated hunting to observational learning, social hierarchy, and courtship—and may be relevant also for the representation of nonconspecific animals—for example, for spatial encoding of predators and prey. These results open many questions for future studies: How are multiple animals represented in the brain? Is there a different representation for socially dominant versus subordinate animals, and for males versus females? These and many other questions await investigation in order to elucidate the neural basis of social-spatial cognition.

REFERENCES AND NOTES

1. J. O'Keefe, L. Nadel, *The Hippocampus as a Cognitive Map* (Oxford Univ. Press, 1978).
2. M. A. Wilson, B. L. McNaughton, *Science* **261**, 1055–1058 (1993).
3. N. Ulanovsky, C. F. Moss, *Nat. Neurosci.* **10**, 224–233 (2007).
4. T. Hafting, M. Fyhn, S. Molden, M.-B. Moser, E. I. Moser, *Nature* **436**, 801–806 (2005).
5. C. Barry, R. Hayman, N. Burgess, K. J. Jeffery, *Nat. Neurosci.* **10**, 682–684 (2007).
6. M. M. Yartsev, M. P. Witter, N. Ulanovsky, *Nature* **479**, 103–107 (2011).
7. J. S. Taube, R. U. Muller, J. B. Ranck Jr., *J. Neurosci.* **10**, 420–435 (1990).
8. A. Peyrache, M. M. Lacroix, P. C. Petersen, G. Buzsáki, *Nat. Neurosci.* **18**, 569–575 (2015).
9. A. Finkelstein *et al.*, *Nature* **517**, 159–164 (2015).
10. T. Solstad, C. N. Boccara, E. Kropff, M.-B. Moser, E. I. Moser, *Science* **322**, 1865–1868 (2008).
11. F. Savelli, D. Yoganarasimha, J. J. Knierim, *Hippocampus* **18**, 1270–1282 (2008).
12. C. Lever, S. Burton, A. Jeewajee, J. O'Keefe, N. Burgess, *J. Neurosci.* **29**, 9771–9777 (2009).
13. G. Neuweiler, *The Biology of Bats* (Oxford Univ. Press, 2000).
14. Materials and methods are available as supplementary materials.
15. M. M. Yartsev, N. Ulanovsky, *Science* **340**, 367–372 (2013).
16. B. E. Pfeiffer, D. J. Foster, *Science* **349**, 180–183 (2015).
17. J. Ferbinteanu, M. L. Shapiro, *Neuron* **40**, 1227–1239 (2003).
18. T. J. Davidson, F. Kloosterman, M. A. Wilson, *Neuron* **63**, 497–507 (2009).
19. A. Sarel, A. Finkelstein, L. Las, N. Ulanovsky, *Science* **355**, 176–180 (2017).
20. S. A. Ho *et al.*, *Neuroscience* **157**, 254–270 (2008).
21. E. J. Henriksen *et al.*, *Neuron* **68**, 127–137 (2010).
22. A. Tsao, M.-B. Moser, E. I. Moser, *Curr. Biol.* **23**, 399–405 (2013).
23. J. J. Knierim, J. P. Neunuebel, S. S. Deshmukh, *Philos. Trans. R. Soc. Lond. B Biol. Sci.* **369**, 20130369 (2013).
24. F. L. Hitti, S. A. Siegelbaum, *Nature* **508**, 88–92 (2014).
25. S. M. Dudek, G. M. Alexander, S. Farris, *Nat. Rev. Neurosci.* **17**, 89–102 (2016).
26. T. Okuyama, T. Kitamura, D. S. Roy, S. Itohara, S. Tonegawa, *Science* **353**, 1536–1541 (2016).
27. L. Zynyuk, J. Huxter, R. U. Muller, S. E. Fox, *Hippocampus* **22**, 1405–1416 (2012).
28. M. von Heimendahl, R. P. Rao, M. Brecht, *J. Neurosci.* **32**, 2129–2141 (2012).
29. X. Mou, D. Ji, *eLife* **5**, e18022 (2016).
30. E. J. Markus *et al.*, *J. Neurosci.* **15**, 7079–7094 (1995).
31. M. A. Moita, S. Rosis, Y. Zhou, J. E. LeDoux, H. T. Blair, *Neuron* **37**, 485–497 (2003).
32. H. Eichenbaum, N. J. Cohen, *Neuron* **83**, 764–770 (2014).
33. G. Rizzolatti, C. Sinigaglia, *Nat. Rev. Neurosci.* **17**, 757–765 (2016).

ACKNOWLEDGMENTS

We thank K. Haroush, S. Romani, O. Forkosh, A. Rubin, M. Geva-Sagiv, A. Finkelstein, T. Eliav, G. Ginosar, A. Sarel, and D. Blum for comments on the manuscript; S. Kaufman, O. Gobi, and S. Futerman for bat training; A. Tuval for veterinary support; C. Ra'anan and R. Eilam for histology; B. Pasmantirer and G. Ankaoua for mechanical designs; and G. Brodsky for graphics. This study was supported by research grants to N.U. from the European Research Council (ERC-CoG–NATURAL_BAT_NAV), Israel Science Foundation (ISF 1319/13), and Minerva Foundation. The data are archived on the Weizmann Institute of Science servers and will be made available on request.

SUPPLEMENTARY MATERIALS

www.sciencemag.org/content/359/6372/218/suppl/DC1
Materials and Methods
Figs. S1 to S8
References (*34*–*42*)
Movies S1 and S2

11 July 2017; accepted 7 December 2017
10.1126/science.aao3474